Available online at www.sciencedirect.com
ScienceDirect
Progress in Nuclear Energy 49 (2007) 120–129
PROGRESS IN NUCLEAR ENERGY
An International Review Journal
www.elsevier.com/locate/pnucene

# Effect of flow rate transients on fission product activity in primary coolant of PWRs

Sikander M. Mirza, M. Javed Iqbal, Nasir M. Mirza*

*Department of Physics & Applied Mathematics, Pakistan Institute of Engineering & Applied Sciences, Nilore, Islamabad 45650, Pakistan*

**Abstract**

Simulations of fission product activity in primary circuits of a typical PWR under flow rate transients have been performed by using a two-stage model for release of fission products from fuel into coolant region. A one-dimensional nodal-scheme has been developed for modeling the behavior of fission products in the primary circuit. For constant-power operation at constant flow rate, results for 15 major fission products show that the activity due to fission products in the primary coolant circuit of PWRs is dominated by $^{133}$Xe and it is followed by $^{135}$Xe, $^{131M}$Xe and $^{129}$Te which contribute 40%, 12.9%, 11% and 8.2%, respectively, to the total fission product activity. The results of these simulations have been found to agree well with the corresponding values found in ANS-18.1 Standard as well as with some available power-plant operation data. These simulations indicate a strong dependence of saturation values of specific activity on primary coolant flow rate. For pump coastdown having a characteristic time $t_p \sim 2000$ h, a 8.6% increase has been observed in the value of total specific activity due to fission products. For increasing $t_p$ values, the value of maximum specific activity due to fission products shows a rise followed by an approach towards a saturation value.


*Keywords:* Fission products; Flow rate transients; Pressurized water reactors; Modeling and simulation

## 1. Introduction

Fuel rod failures do occur during normal operation of reactors and the detection of failed fuel is one of the most important issues in routine PWR operation (Seixas et al., 2001). It has strong implications on reactor performance as well as on safe operation of power plants. The grid fretting, debris, fabrication issues, crud/corrosion, handling damage, clad creep etc., are currently dominant contributors towards fuel failure. This problem is aggravated by current trend towards longer fuel cycle length as well as high burnup cores (Millett and Wood, 1997). Both of these factors translate into higher stresses and consequently higher rates of stress corrosion cracking leading to higher fuel failure rates.

The fuel failure not only increases the occupational radiation level during normal operation, but the routine repair and maintenance are also affected by it resulting in delay and prolongation of maintenance schedules. The corresponding economic penalties have been estimated to be of the order of several million dollars annually. Additionally, necessary steps are required for removal, transport and treatment of the failed fuel which also entail economic

* Corresponding author. Tel.: +92 51 92902724; fax: +92 51 9223727.
*E-mail address:* nasirmm@yahoo.com (N.M. Mirza).

0149-1970/$ - see front matter © 2006 Elsevier Ltd. All rights reserved.
doi:10.1016/j.pnucene.2006.10.001

repercussion. While the root cause investigation has shown a decreasing trend in fuel failure rates over past quarter century, the problem still persists. As shown in Fig. 1 (EPRI, 2002), for LWRs in the United States alone, an annual rate of 0.5–1.5 failed fuel assemblies/GW(e) is reported (Ozer, 1994). A considerable fraction of these failure rates is attributed to unknown causes. New fuel fabrication technologies, having reduced susceptibility of failed fuel rods towards secondary degradation, are being evaluated.

The primary coolant activity is constituted by primary coolant activation, corrosion products and fission products. A number of recent studies have been performed (Mirza et al., 2003, 2005; Rafique et al., 2005) on transient behavior of corrosion product activity in primary circuits of PWRs. These included the modeling and simulation of activation, deposition, and re-release of corrosion products in these systems.

In past, much research effort has been made for the estimation of failed fuel rods by using the primary coolant activities (Kreider and Schneider, 1990; Turnage et al., 1994). Both experimental as well as theoretical techniques have been developed for this purpose. On the experimental side, automated non-destructive methods of leakage detection have been receiving an increasing attention (Kreider and Schneider, 1990). Currently, nuclear reactors are equipped with online coolant activity monitors which utilize gamma-ray spectrometers for quantification of radioactive releases. The online system normally carries out measurement of Xe-133 gas and possible interference from the mixed-in N-13 is removed by anti-coincidence technique. Alternatively, online chemical analysis of sampled primary coolant is used for failed fuel analysis. Recently, the ultrasound pulse-echo inspection technique combined with matched filters' technique has been developed (Seixas et al., 2001) which has false alarm probability smaller than 3%.

The data obtained from online radioactivity measurements are used in various computer programs including IODYNE (Clink and Freeburn, 1987) for estimation of failed fuel rods. These codes are typically based on empirical failure models including general as well as combined failure models which are applicable at high-power and low-power failures correspondingly. However, these codes consistently tend to underestimate the number of failed fuel rods (Lambert et al., 1996). Furthermore, the off-line estimation codes are designed for steady-state, constant-power analysis which restricts their usefulness to non-transient domain.

In this work, a kinetic model is presented for the simulation of fission product activity in primary circuit of a typical PWR which is applicable to both steady state as well as transient regimes. The predictions of this kinetic model with the available power-plant data for steady-state operation have been compared in this work. Results for the dependence of saturation value of fission product activity on flow rate are included. The time behavior of fission product activity in

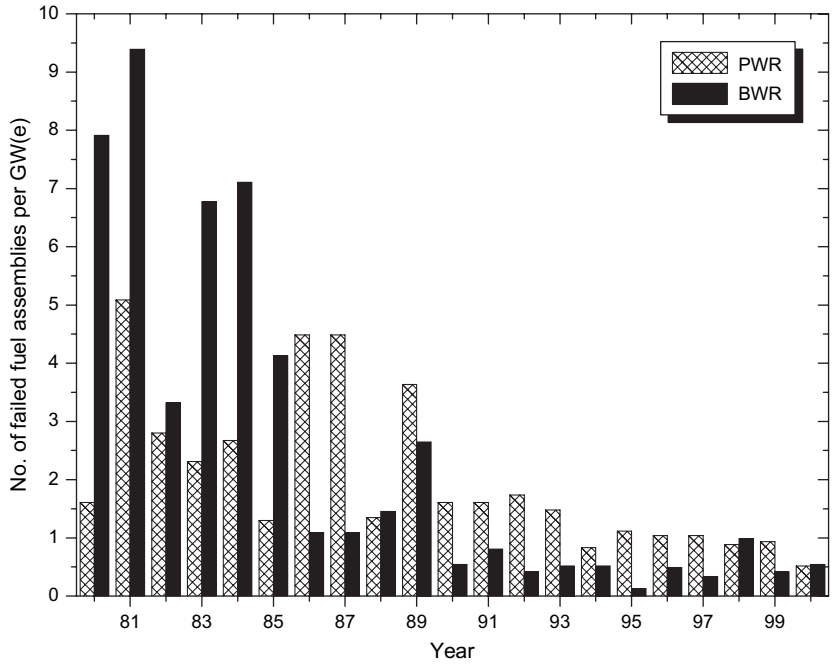


Fig. 1. Trend of US fuel failure rates for boiling water reactor (BWRs) and pressurized water reactors (PWRs) over a 20-year period.

the case of pump coastdown has been studied for both fast as well as for slow coastdown scenario. The dependence of maximum value of total activity due to fission products on the pump coastdown characteristic time has also been studied and the corresponding results are presented (Fig. 2).

## 2. Mathematical model

### 2.1. Kinetics of fission product activity

A typical 300 MWe PWR has been considered operating at constant power in these studies. Table 1 shows some of the design specifications of such a system. For modeling the fission product inventory in the fuel, the standard equations have been extended (Chun et al., 1998) as:

$$\frac{dN_{F,i}}{dt} = FY_iP + \sum_{j=1}^{i-1} f_{ij}\lambda_j N_{F,j} - (\lambda_i + \nu_i + \sigma_i\phi)N_{F,i}; \quad i = 1,2,3,4 \tag{1}$$

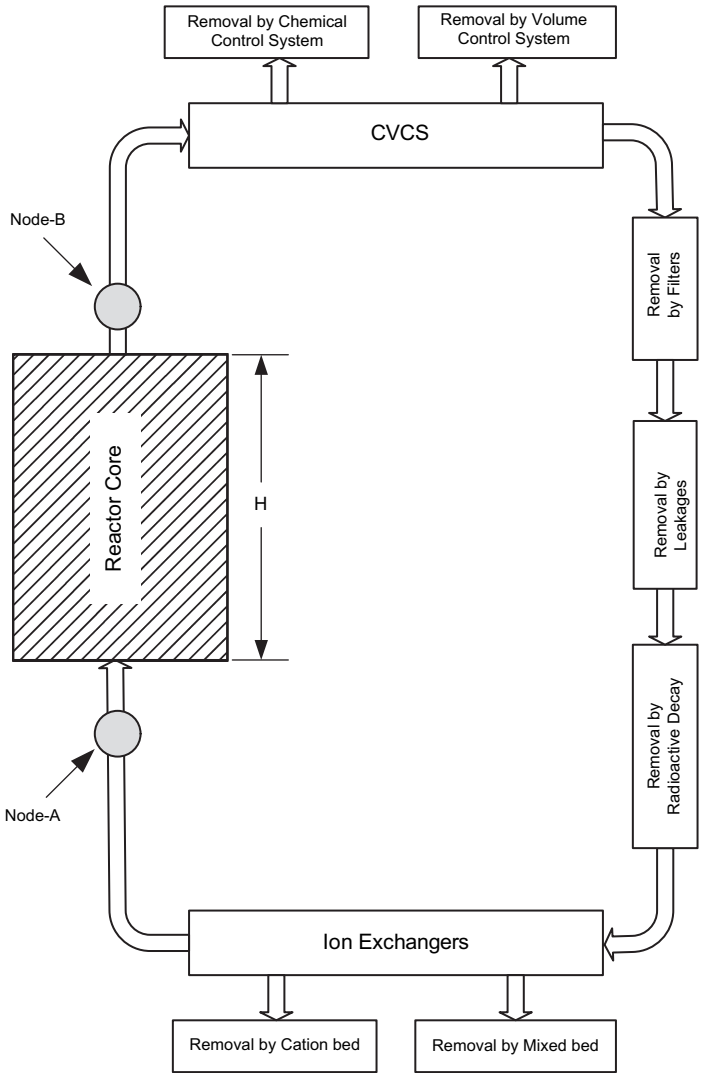


Fig. 2. Schematic diagram of production and loss cycle of fission product activity in primary coolant circuit of PWRs.

Table 1
The design parameters of a typical PWR system (Glasstone and Sesonske, 1994)

| Parameter | Value |
|---|---|
| Specific power ($MW_{th}$/kg U) | 33 |
| Power density ($MW_{th}/m^3$) | 102 |
| Core height (m) | 4.17 |
| Core diameter (m) | 3.37 |
| No. of fuel assemblies | 194 |
| Rods per assembly | 264 |
| Fuel type | $UO_2$ |
| Clad type | Zircoloy |
| Lattice pitch (mm) | 12.6 |
| Fuel rod outer diameter (mm) | 9.5 |
| Average enrichment (w%) | 3.0 |
| Flow rate (Mg/s) | 18.3 |
| Linear heat rate ($kW/m^2$) | 17.5 |
| Coolant pressure (MPa) | 15.5 |
| Inlet coolant temperature (°C) | 293 |
| Outlet coolant temperature (°C) | 329 |

where, $N_{F,i} \equiv$ No. of $i$th radionuclide atoms in fuel (indicated by subscript F), $F \equiv$ average fission rate (fissions/W s), $Y_i \equiv$ fission yield of the $i$th radionuclide, $f_{ij} \equiv i \rightarrow j$ branching ratio, $\sigma_i \equiv$ microscopic abs. cross section for the $i$th radionuclide ($cm^2$), $\nu_i \equiv$ escape rate coefficient for the $i$th radionuclide, $\lambda_i \equiv$ decay constant of the $i$th radionuclide, and $P \equiv$ reactor core thermal power (W); and in the gap region:

$$\frac{dN_{G,i}}{dt} = \nu_i N_{F,i} + \sum_{j=1}^{i-1} f_{ij}\lambda_j N_{G,j} - (\lambda_i + D\varepsilon_i + \sigma_i\phi)N_{G,i}; \quad i = 1,2,3,4 \tag{2}$$

with, $N_{G,i} \equiv$ No. of $i$th radionuclide atoms in fuel-clad gap (indicated by subscript G), $D \equiv$ failed fuel fraction, and $\phi \equiv$ neutron flux (#/$cm^2$ s).

For a constant-power operation, Eqs. (1) and (2) yield the following:

$$N^*_{F,i} = \frac{FY_iP + \sum_{j=1}^{i-1} f_{ij}\lambda_j N^*_{F,j}}{(\lambda_i + \nu_i + \sigma_i\phi)}, \quad i = 1,2,3,4 \tag{3}$$

and

$$N^*_{G,i} = \frac{\nu_i N^*_{F,i} + \sum_{j=1}^{i-1} f_{ij}\lambda_j N^*_{G,j}}{(\lambda_i + D\varepsilon_i + \sigma_i\phi)}, \quad i = 1,2,3,4 \tag{4}$$

where, the asterisks represent the corresponding time-independent values for constant-power operation.

For the modeling of transient behavior of fission product activity in the coolant, a one-dimensional model of reactor has been used as shown in Fig. 1. The values of fission product activity at two nodes, one at the core inlet (node A) and the other at core outlet point (node B) at any time, are governed by the following coupled set of equations:

$$N^B_{C,i}(t) = N^A_{C,i}(t)[\exp(-\lambda_i\Delta t_{AB}) - \sigma_i\phi\Delta t_{AB}V_{w,c}] + \frac{\lambda D\varepsilon_i N^*_{G,i}\Delta t_{AB}}{V_{w,c}\rho}\exp(-\lambda_i\Delta t_{AB}) + \sum_{j=1}^{i-1} f_{ij}N^B_{C,j}(t)\{1 - \exp(-\lambda_i\Delta t_{AB})\}, \quad i = 1,2,3,4 \tag{5}$$

and

$$N^{A}_{C,i}(t) = N^{B}_{C,i}(t)\left[1 - \left\{\frac{Q}{W}\eta_i + \beta + \frac{L}{W}\right\}\right]\exp(-\lambda_i \Delta t_{BA}) + \sum_{j=1}^{i-1} f_{ij} N^{B}_{C,j}(t)\{1 - \exp(-\lambda_i \Delta t_{BA})\}, \quad i = 1,2,3,4 \qquad (6)$$

where, $\Delta t_{AB} = H/V_{w,c}$ is the time taken by coolant to move from node A to node B, $H$ is the core height and $V_{w,c}$ is the coolant speed within the core region; $\Delta t_{BA} = L/V_{w,o}$ is the time taken by the coolant to move from node B to A, $L$ is the outer segment length of primary circuit, and $V_{w,o}$ is the coolant speed in this outer segment. Also, we have $N_{C,i} \equiv$ No. of $i$th radionuclide atoms in primary coolant (indicated by subscript C), $\beta \equiv$ bleed-out fraction for boron control, $L \equiv$ coolant leakage rate (g/s), $w \equiv$ total coolant mass (g), $\eta_i \equiv$ resin purification efficiency for $i$th radionuclide, and $Q \equiv$ let-down flow rate (g/s).

Tables 2 and 3 give the values of various parameters used in these simulations.

### 2.2. Pump coastdown model

The primary pump coastdown is modeled by equating the frictional retarding force to the changes in the momentum of the fluid. For a specific value of velocity ($v$) and fluid density ($\rho$), the resulting balance equation is (Lewis, 1977)

$$\frac{L\rho}{g_c}\frac{dv}{dt} = -C_f\frac{\rho v^2}{2g_c} \qquad (7)$$

where, $L$ is the total length of the loop and $C_f$ is the total pressure loss coefficient for the loop. The solution in terms of flow rate is

$$w(t) = \frac{w_0}{(1 + t/t_p)} \qquad (8)$$

In Eq. (8), $w_0$ is the steady-state value of flow rate available at the start of pump coastdown and the characteristic time '$t_p$' has value $2L/C_f v_0$. For this study, a large enough value of $t_p$ ($\sim$2000 h) has been used in order to avoid the boiling crisis until after the reactor trip.

## 3. Simulation results

The study of fission product activity in primary circuits has been carried out based on a typical PWR (Glasstone and Sesonske, 1994) and the corresponding design specifications are given in Table 1. The values of various operational parameters used in these simulations are given in Table 2. These include the value's various parameters such as failed fuel fraction, coolant leakage rate, resin purification efficiency and primary coolant bleed-out fraction for boron control. The essential data for various fission products and their progeny are given in Table 3. This includes half-lives, yields and branching ratios etc.

Table 2
Values of various operational parameters used in these simulations

| Parameter | Value |
|---|---|
| $D$ | $2.5 \times 10^{-3}$ |
| $L$ (g/s) | 2.3 |
| $Q$ (g/s) | 470 |
| $\beta$ | 0.001 |
| $W$ (g) | $1.072 \times 10^{9}$ |
| $V$ (cm$^3$) | $1.485 \times 10^{9}$ |
| $\tau$ | 0.056 |
| $P_o$ (MW$_{th}$) | 998 |
| $F$ (fission/W s) | $3.03 \times 10^{10}$ |

Table 3
Data for various fission product gases and associated decay products

| Isotope (location in chain) | $T_{1/2}$[a] | $\eta$ | $Y$[b] | $\nu$ | $\sigma$ (b)[b] | Branching ratios, $f_{ij}$ | | | | |
|---|---|---|---|---|---|---|---|---|---|---|
| | | | | | | 1 → 2 | 1 → 3 | 2 → 3 | 2 → 4 | 3 → 4 |
| $^{85M}$Kr (1) | 4.48 h | 0.4538 | 1.3E−2 | 6.5E−8 | 0.0 | 1.0 | 0.0 | | | |
| $^{85}$Kr (2) | 10.752 y | 3.958E−5 | 1.3E−2 | 6.5E−8 | 1.84E−1 | | | 1.0 | | |
| $^{87}$Kr (3) | 1.272 h | 0.7454 | 2.56E−2 | 6.5E−8 | 5.518E+1 | 1.0 | | | | |
| $^{88}$Kr (1) | 2.84 h | 0.5674 | 3.55E−2 | 6.5E−8 | 0.0 | 1.0 | 0.0 | | | |
| $^{129}$Te (3) | 1.16 h | 0.9 | 5.11E−3 | 1.0E−9 | 0.0 | | | | 0.37 | |
| $^{129}$I (4) | 1.61E7 y | 0.99 | 5.0E−6 | 1.3E−8 | 5.225 | | | | | 1.0 |
| $^{131M}$ Te (1) | 1.25 d | 0.9 | 1.1E−2 | 1.0E−9 | 0.0 | 0.21 | 0.79 | | | |
| $^{131}$Te (2) | 25.0 m | 0.9 | 1.71E−2 | 1.0E−9 | 0.0 | | | 1.0 | 0.0 | |
| $^{131}$I (3) | 8.023 d | 0.99 | 3.29E−5 | 1.3E−8 | 3.229E−1 | | | | | 0.0109 |
| $^{131M}$Xe (4) | 11.93 d | 8.923E−3 | 4.05E−4 | 6.5E−8 | 0.0 | | | | | |
| $^{132}$I (4) | 2.28 h | 0.99 | 2.06E−4 | 1.3E−8 | 0.0 | | | | | |
| $^{133}$I (2) | 20.8 h | 0.99 | 4.9E−2 | 1.3E−8 | 0.0 | | | 0.0285 | 0.9715 | |
| $^{133M}$Xe (3) | 2.19 d | 4.663E−2 | 2.67E−5 | 6.5E−8 | 0.0 | | | | | 1.0 |
| $^{133}$Xe (4) | 5.244 d | 2.001E−2 | 4.9E−02 | 6.5E−8 | 2.44E+1 | | | | | |
| $^{134}$I (2) | 52.8 m | 0.99 | 7.83E−2 | 1.3E−8 | | | | 1.0 | 0.0 | |
| $^{135}$I (2) | 6.57 h | 0.9 | 2.98E−2 | 1.3E−8 | 2.119E−3 | | | 0.1651 | 0.8349 | |
| $^{135M}$Xe (3) | 15.29 m | 0.9098 | 1.10E−2 | 6.5E−8 | 0.0 | | | | | 0.994 |
| $^{135}$Xe (4) | 9.14 h | 0.2205 | 6.54E−2 | 6.5E−8 | 2.445E+5 | | | | | |

[a] Croff, 1980.
[b] JEFF 3.1, 2005.

These simulations have been carried out by taking reactor at constant full power with zero fission product activity in primary coolant at $t = 0$. Fifteen dominant fission products have been used in these simulations including $^{133}$Xe, $^{85}$Kr, $^{131}$I, $^{135}$I and $^{129}$Te. The time variation of various fission product activities in primary coolant is shown in Fig. 3. The $^{133}$Xe is dominant contributor towards fission product activity coolant. Nearly 40% of the total fission product activity is produced by it while $^{135}$Xe, $^{131M}$Xe, $^{129}$Te contribute 12.9%, 11% and 8.2%, respectively. The simulated saturation

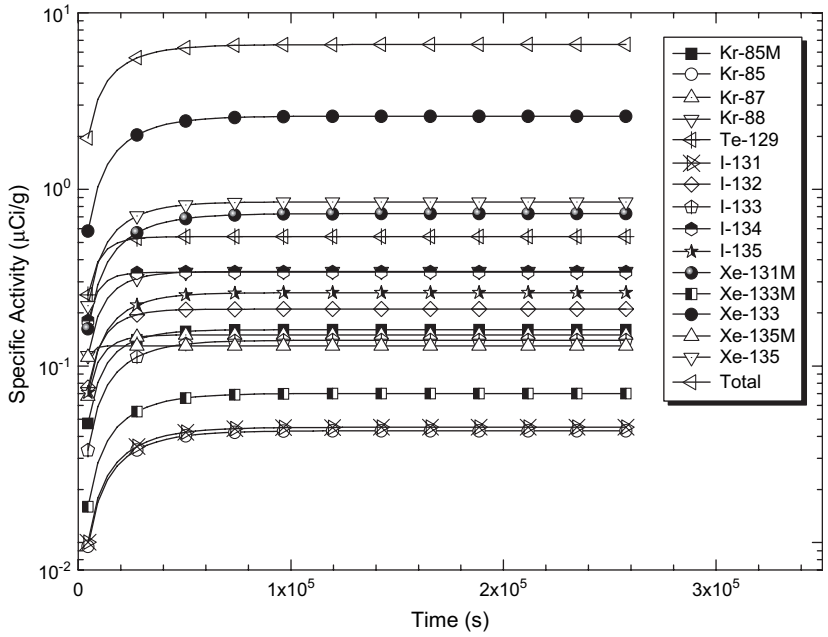


Fig. 3. Approach to saturation values of specific activities for various fission products at constant values of reactor power and primary coolant flow rate.

values of fission product activity for various isotopes have been found in good agreement with corresponding data measured/standard data available in literature as shown in Table 4.

The dependence of saturation values of specific fission product activity on primary coolant flow rate has been carried out and the results are shown in Fig. 4. For increasing flow rate, a decreasing trend is seen for the saturation values of fission product activity due to various radioisotopes. The sensitivity analysis shows that in the neighborhood of normal flow rate, for total saturation specific activity, the value of sensitivity coefficient is

$$\frac{dA_{sat,T}}{dF} = -2.596 \times 10^{-7}\ \mu Ci/s \tag{9}$$

It has a value of $-6.1 \times 10^{-4}$ μCi/s at lower flow rates and tends to approach a value of $-0.393 \times 10^{-7}$ μCi/s for high flow rate.

In the case of pump coastdown, the reactor is operating at full power at normal flow rate at the time when the coastdown starts. Due to decrease in flow rate, the specific activities due to various fission products exhibit an increasing trend as shown in Fig. 5. The total specific fission product activity shows 8.6% increase before reactor shutdown gets initiated due to low-flow signal initiated at 90% of nominal flow.

For pump coastdown, the response of primary coolant specific activity due to fission products depends on the characteristic time '$t_p$'. This dependence has been shown in Fig. 6. It is clear from this figure that the maximum value of the total specific activity attained increases by increasing the value of '$t_p$'. The value of rate of increase of the total specific activity with increase in '$t_p$' has the following value:

$$\frac{dA_{max,T}}{dt_p} = 7 \times 10^{-6}\ \mu Ci/g\ h \tag{10}$$

The variation of the maximum total fission product specific activity with the pump coastdown characteristic time '$t_p$' is shown in Fig. 7. The simulations indicate initially a rising trend which is followed by an approach towards a saturation value (~7.2 μCi/g). This is consistent with the expectation that for larger values of '$t_p$', it requires longer time before reactor scram occurs and during this time a higher value of total specific activity will be reached. The converse is also true for small '$t_p$' values.

Table 4
Comparison of the calculated values of specific activity of various isotopes in primary coolant of a typical PWR with the ANS-18.1 Standard and some experimentally measured data

| Isotope | $\varepsilon$ ($s^{-1}$) | This work (μCi/g) | ANS-18.1 (μCi/g)[a] | Measured (μCi/g) | | | | |
|---|---|---|---|---|---|---|---|---|
| | | | | Surry Unit-1[b] | Turkey point Unit-3[c] | Turkey Point Unit-4[c] | H.B. Rob. Unit-2[b] | R.E. Ginna-Plant[b] |
| $^{85M}$Kr | 0.005 | 1.62E−1 | 1.6E−1 | | 1.8E−2 | 1.7E−2 | 7.94E−3 | 0.08 |
| $^{85}$Kr | 0.005 | 4.58E−2 | 4.3E−1 | 2.01E−1 | | <8.0E−4 | | |
| $^{87}$Kr | 1.0E−3 | 1.49E−1 | 1.5E−1 | 7.86E−4 | 3.4E−2 | 2.5E−2 | 6.74E−3 | 0.20 |
| $^{88}$Kr | 4.5E−3 | 2.74E−1 | 2.8E−1 | | 4.7E−2 | 3.8E−2 | 9.45E−3 | 0.22 |
| $^{129}$Te | 2.5E−3 | 1.10E−2 | | | 1.0E−2 | <1.0E−2 | | |
| $^{131}$I | 6.0E−5 | 4.21E−2 | 4.5E−2 | 8.26E−4 | 1.1E−2 | 8.0E−3 | 2.07E−3 | 0.07 |
| $^{132}$I | 4.5E−3 | 2.08E−1 | 2.1E−1 | | 1.4E−1 | 1.9E−2 | 1.49E−2 | 0.79 |
| $^{133}$I | 7.0E−4 | 1.50E−1 | 1.4E−1 | 4.89E−3 | 8.8E−2 | 1.7E−2 | 8.40E−3 | 0.46 |
| $^{134}$I | 1.5E−2 | 3.32E−1 | 3.4E−1 | 1.17E−3 | 2.6E−1 | 2.2E−2 | 3.03E−2 | 1.24 |
| $^{135}$I | 5.0E−3 | 2.12E−1 | 2.6E−1 | 5.20E−3 | 1.5E−1 | 1.9E−2 | 2.14E−2 | 0.75 |
| $^{131M}$Xe | 0.8 | 3.94E−2 | 7.3E−1 | | <2.0E−3 | 3.0E−4 | | |
| $^{133M}$Xe | 1.5E−3 | 7.02E−2 | 7.0E−2 | | 4.3E−3 | 6.6E−3 | 3.28E−3 | |
| $^{133}$Xe | 3.4E−4 | 2.60 | 2.60 | 1.42E−2 | 2.0E−1 | 2.1E−1 | 1.75E−1 | 1.28 |
| $^{135M}$Xe | 2.0E−2 | 1.25E−1 | 1.3E−1 | | 1.1E−1 | 2.1E−2 | | 0.12 |
| $^{135}$Xe | 3.5E−3 | 8.20E−1 | 8.5E−1 | | 1.5E−1 | 1.2E−1 | 3.82E−2 | 0.81 |

[a] ANSI/ANS-18.1, 1984.
[b] WCAP-8253, May 1974 (Westinghouse Electric Co., 1974).
[c] NUREG/CR-1992 (Mandler et al., 1981).

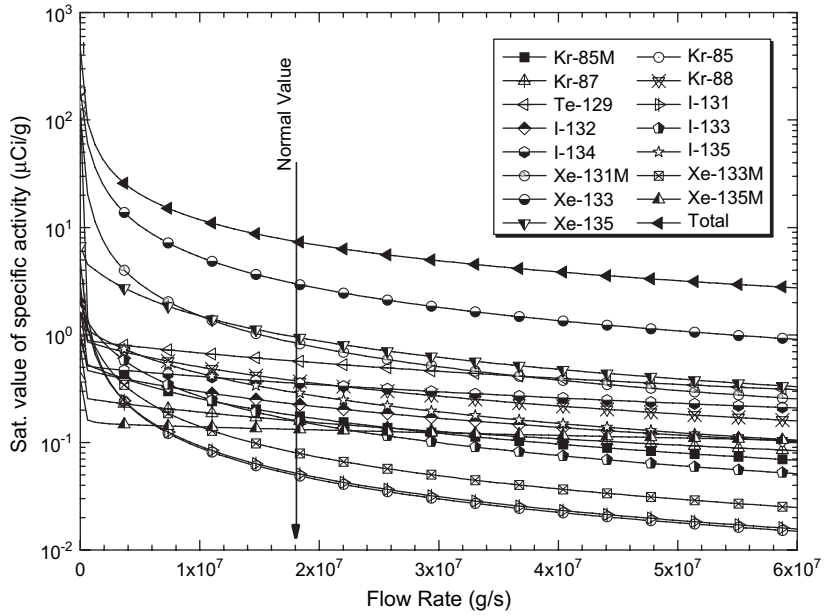


Fig. 4. Dependence of saturation values of specific activities of various fission products on primary coolant flow rate at constant reactor power.

## 4. Conclusions

- Transient behavior of fission product activity under flow rate perturbations has been studied in this work. The release of fission products from fuel into the primary coolant has been modeled as a two-stage process. The time dependence of fission product activity in the primary coolant has been studied using nodes along a one-dimensional primary circuit model.

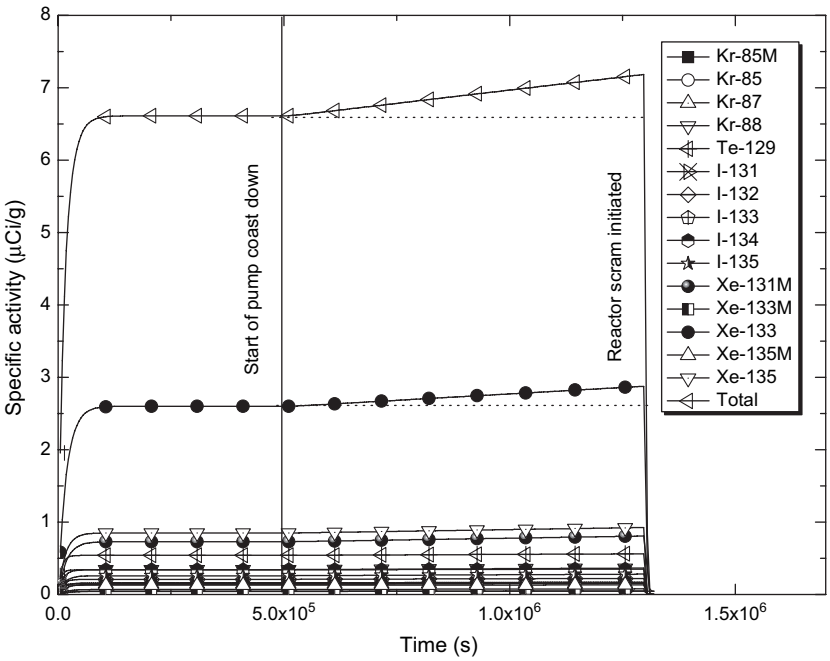


Fig. 5. Time variation of specific activities of various fission products for pump coastdown at constant reactor power.

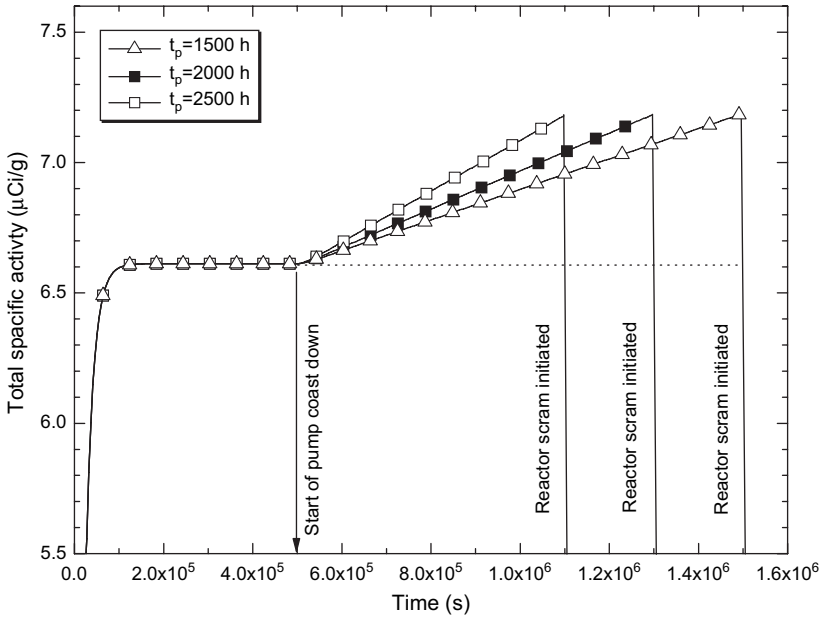


Fig. 6. Transient response of the total specific activity for pump coastdown for the three indicated values of the characteristic time $t_p$.

- Results for 15 dominant fission products for constant-power operation at normal flow rate show a rapid rise of the specific fission product activity towards saturation. The value of specific activity is dominated by $^{133}$Xe, $^{135}$Xe, $^{131M}$Xe and $^{129}$Te which contribute 40%, 12.9%, 11% and 8.2%, respectively, of the total specific activity.
- The simulations show strong dependence of primary coolant activity on prevailing flow rate. By increasing the value flow rate, the saturation values of specific activity due to various fission products show a decreasing trend.
- For normal conditions, the pump coastdown (with $t_p \sim 2000$ h) results in 8.6% increase of total specific activity due to fission products. This maximum value of the total specific activity has been found to exhibit a rise followed by an approach towards saturation value as the value of the coastdown characteristic time is increased.

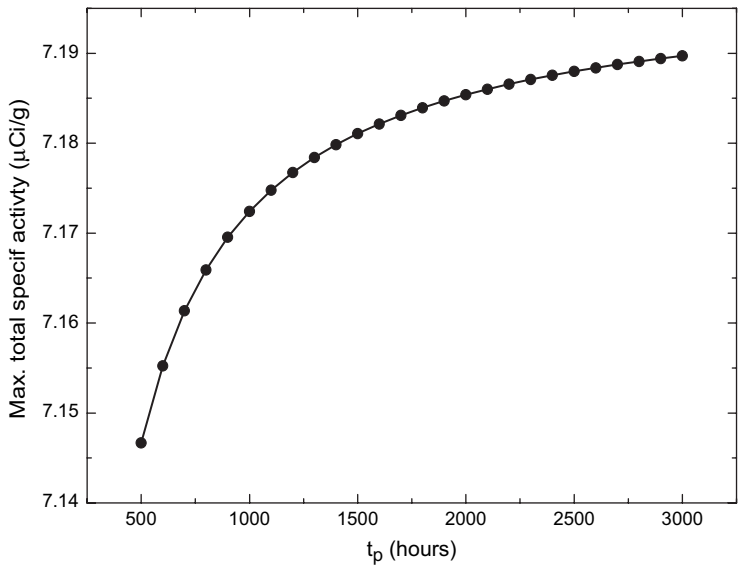


Fig. 7. Dependence of the maximum attained values of the total specific activities on the pump coastdown characteristic time $t_p$.

## Acknowledgement

M. Javed Iqbal gratefully acknowledges the financial support from the Higher Education Commission (HEC), Pakistan for the Ph.D. (Indigenous) fellowship under Grant # 17-6(118)Sch/2002/Phase-II.

## References

ANSI/ANS-18.1, 1984. Radioactive source term for normal operation of light water reactors.

Chun, M.H., Tak, N.I., Lee, S.K., 1998. Development of a computer code to estimate the fuel rod failure using primary coolant activities of operating PWRs. Ann. Nucl. Energy 25 (10), 753–763.

Clink, L., Freeburn, H., 1987. Estimating PWR fuel rod failures throughout a cycle. Trans. Am. Nucl. Soc. 54 (1), 13.

Croff, A.G., 1980. A User's Manual for the ORIGEN Computer Code. Oak Ridge National Laboratory, Oak Ridge.

EPRI Report, 2002. In: WG4 Project Status: Robust Fuel Program, 12–13 February, Las Vegas, Nevada.

Glasstone, S., Sesonske, A., 1994. Nuclear Reactor Engineering, fourth ed., vol. 1. Chapman and Hall.

JEFF 3.1, 2005. Joint evaluated nuclear data library for fission and fusion applications. NEA Data Bank, AEN, NEA.

Kreider, S.D., Schneider, A., 1990. The detection of failed fuel in LWRs: a historical review. Trans. Am. Nucl. Soc. 61, 46–47.

Lambert, J.D.B., Gross, K.C., Depiante, E.V., 1996. Adaptation of gas tagging for failed fuel identification in light water reactors. In: Proceedings of ASME Fourth International Conference on Nuclear Engineering, CONF-960306-25.

Lewis, E.E., 1977. Nuclear Power Reactor Safety. John Wiley, New York.

Millett, P.J., Wood, C.J., 1997. Recent advances in water chemistry control at US PWRs. In: EPRI, Proceedings of 58th International Water Conference, Pittsburgh.

Mirza, N.M., Rafique, M., Hyder, M.J., Mirza, S.M., 2003. Computer simulation of corrosion product activity in primary coolants of a typical PWR under flow rate transients and linearly accelerated corrosion. Ann. Nucl. Energy 30, 831–851.

Mirza, N.M., Rafique, M., Mirza, S.M., Hyder, M.J., 2005. Simulation of corrosion product activity for nonlinearly rising corrosion on inner surfaces of primary coolant pipes of a typical PWR under flow rate transients. Appl. Radiat. Isot. 62, 681–692.

Mandler, J., Stalker, A., Croney, S., Mclsaac, C., Soli, G., Hartwell, J., Loret, L., Motes, B., Cox, T., Akers, D., Bihl, N., Duce, S., Tkachyk, J., Pelletier, C., Voilleque, P., 1981. In-plant source term measurements at four PWRs, NUREG/CR-1992 RR.

Ozer, O., 1994. Overview of U.S. utility experience with identification and disposition of failed LWR fuel. Trans. ANS 70, 72.

Rafique, M., Mirza, N.M., Mirza, S.M., 2005. Kinetic study of corrosion product activity in primary coolant pipes of a typical PWR under flow rate transients and linearly increasing corrosion rates. J. Nucl. Mater. 346, 282–292.

Seixas, J.M., Freeland, F.P., Soares-Filho, W., 2001. Matched filters for identifying failed fuel rods in nuclear reactors. In: Proceedings of the IEEE International Conference on Electronics, Circuits and Systems, 2–5 September 2001, Sant Julians, Malta, vol. 2, pp. 643–646.

Turnage, K.G., Hunt, B.E., Bennertt, S.D., Gibson, E.B., 1994. Fission product analysis and operational experience with leaking fuel rods at hatch nuclear plant. In: Proceedings of International Topical Meeting on LWR Fuel Performance, American Nuclear Society. pp. 467–476.

Westinghouse Electric Co., 1974. Nuclear energy systems: source term data for Westinghouse PWRs, WCAP-8253.